frontiers in Earth Science

ORIGINAL RESEARCH
published: 12 February 2021
doi: 10.3389/feart.2021.635181

High-Resolution Stable Isotope Paleotopography of the John Day Region, Oregon, United States

Tyler Kukla[1]*, *Daniel Enrique Ibarra*[1,2,3], *Jeremy K. Caves Rugenstein*[4], *Jared T. Gooley*[1,5], *Casey E. Mullins*[6], *Samuel Kramer*[7], *Danielle Y. Moragne*[7,8] and *C. Page Chamberlain*[1]

[1]Department of Geological Sciences, Stanford University, Stanford, CA, United States, [2]Institute at Brown for Environment and Society and the Department of Earth, Environmental and Planetary Science, Brown University, Providence, RI, United States, [3]Department of Earth and Planetary Science, University of California, Berkeley, Berkeley, CA, United States, [4]Department of Geosciences, Colorado State University, Fort Collins, CO, United States, [5]Currently at United States Geological Survey, Reston, VA, United States, [6]Earth Systems Program, Stanford University, Stanford, CA, United States, [7]Department of Earth System Science, Stanford University, Stanford, CA, United States, [8]Department of Earth Sciences, Dartmouth College, Hanover, NH, United States

OPEN ACCESS

Edited by:
Heiko Pingel,
University of Potsdam, Germany

Reviewed by:
Gregory Retallack,
University of Oregon, United States
John Bershaw,
Portland State University,
United States

***Correspondence:**
Tyler Kukla
tykukla@stanford.edu

Specialty section:
This article was submitted to Quaternary Science, Geomorphology and Paleoenvironment, a section of the journal Frontiers in Earth Science

Received: 30 November 2020
Accepted: 14 January 2021
Published: 12 February 2021

Citation:
Kukla T, Ibarra DE, Rugenstein JKC, Gooley JT, Mullins CE, Kramer S, Moragne DY and Chamberlain CP (2021) High-Resolution Stable Isotope Paleotopography of the John Day Region, Oregon, United States. Front. Earth Sci. 9:635181. doi: 10.3389/feart.2021.635181

The John Day region of central Oregon, United States contains ~50 million years of near-continuous, fossiliferous sedimentation, representing one of the world's richest archives of Cenozoic terrestrial ecosystems and climate. Stable isotope proxy data from this region are commonly used to infer the elevation history of the Cascades, which intercept westerly moisture in transit to the John Day region. However, the Blue Mountains, which accreted in the Mesozoic, create a region of local high topography that can confound signals of Cascades uplift. John Day deposits, including the John Day Formation, are divided into an eastern facies located within the Blue Mountains and a western facies in the adjacent plains. As a result, the Blue Mountains may have supported gradients in climate and ecology between the eastern and western facies, and constraining these gradients is necessary for reconstructing past topography and ecosystem change. In order to define the Cenozoic extent and magnitude of Blue Mountains topography we use oxygen isotopes in authigenic clay minerals to construct a spatially resolved map of local elevation. We find that the oxygen isotope composition of clay minerals within the Blue Mountains is ~3‰ lower than in the adjacent high plains, and this offset is mostly constant throughout our record (spanning ~50 – 5 Ma). We attribute this offset to Blue Mountains topography, either directly from upslope rainout or indirectly through the effect of elevation on local variations in precipitation seasonality. Our results highlight the importance of local topographic features in regional paleotopography reconstructions and provide important biogeographical context for the rich paleo-floral and -faunal records preserved in John Day sediments.

Keywords: paleotopography, John Day, Blue Mountains, oxygen isotopes, biogeography, clay minerals

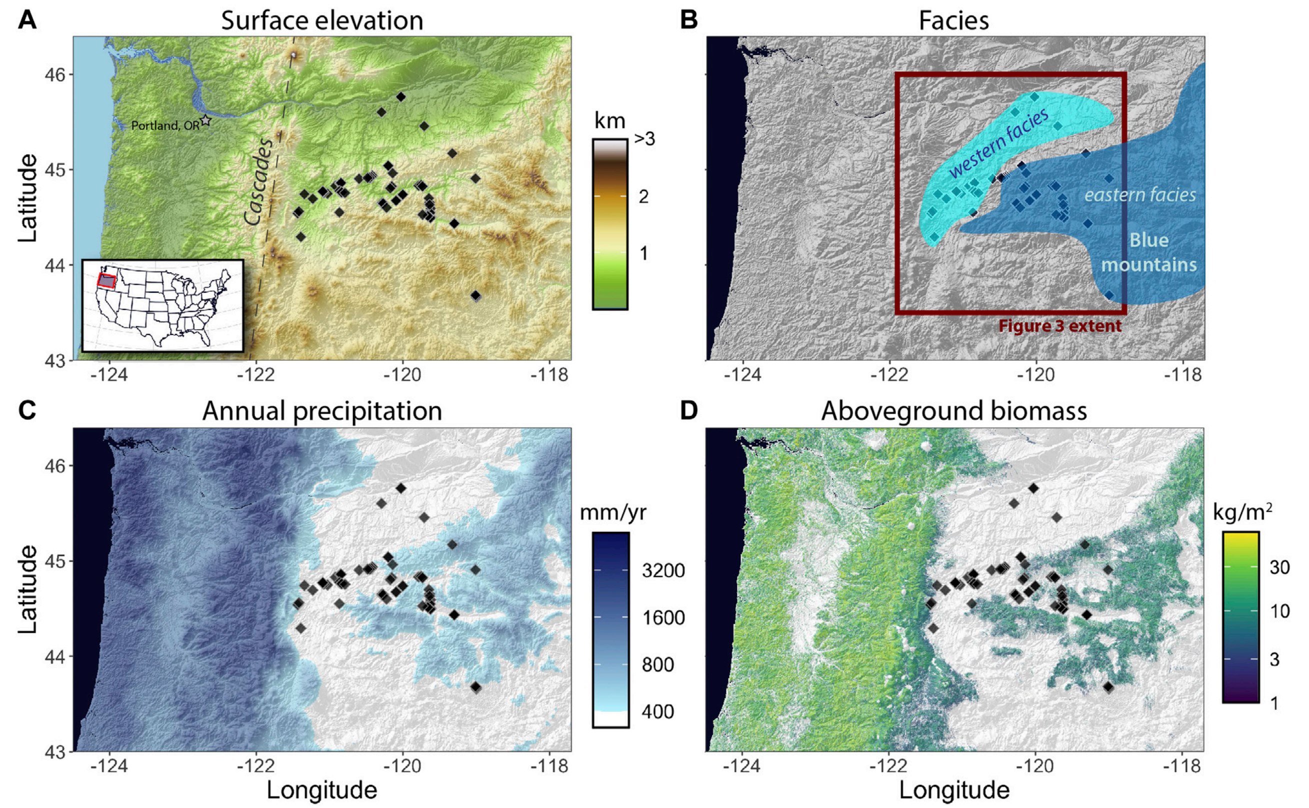

FIGURE 1 | (A) Surface elevation (km) map of study region. Light blue represents ocean, diamond symbols are authigenic clay sample locations. Inset indicates the location of the study area within the United States. Elevation data collected with the elevatr package in R. **(B)** Approximate extent of the western (light blue polygon) and eastern (dark blue polygon) facies. Eastern facies follows the extent of the Blue Mountains region. Polygons based on Albright et al. (2008); Graham (2014); Robinson et al. (1984); Takeuchi (2007). Red box denotes the areal extent of maps in **Figure 3**. **(C)** Annual precipitation map (mm/yr). White area receives less than 400 mm of precipitation per year and characterizes the Cascades rainshadow. Data from the PRISM Climate Group (2012). **(D)** Aboveground biomass (kg/m^2; live, dry). White area denotes no or negligible aboveground biomass. Data from Kellndorfer et al. (2012).

INTRODUCTION

The John Day region lies in the High Desert of central Oregon with the Cascades Range to the west and the Blue Mountains province to the east (**Figures 1A,B**). The region, denoted here as the extent of the eastern and western facies (**Figure 1B**), is known for its near-continuous, fossil-rich terrestrial sedimentation, making it one of the planet's most complete records of Cenozoic environments and climate. Over one hundred years of extensive study has built a foundation ripe for disentangling the co-evolution of local climate, landscapes, and life (Bestland and Retallack, 1994; Clark, 1989; Dillhoff et al., 2009; Merriam and Sinclair, 1906; Retallack et al., 2004; Robinson et al., 1984; Robson et al., 2019; Samuels et al., 2015; Sinclair, 1905; Swanson and Robinson, 1968). In addition to providing an ideal case study for paleo-biogeographical change (Kohn and Fremd, 2007; Retallack, 2004), John Day proxy data have been used to unravel the tectonic history of the Cascades, which serve as a barrier between Oregon's High Desert and moisture-laden winter westerly winds originating in the Pacific (Bershaw et al., 2019; Kohn et al., 2002; Takeuchi et al., 2010). Due to the strong rainshadow cast by the Cascades today (**Figure 1C**), the range's uplift history is considered an important driver of Cenozoic precipitation and vegetation change in the John Day region and across the northwestern United States (Retallack, 2004; Takeuchi and Larson, 2005; Kohn and Fremd, 2007; Takeuchi et al., 2010).

However, the Cascades Range is not the only topographic feature of consequence in the John Day region. The Blue Mountains province, which accreted in the Mesozoic (Dickinson and Thayer, 1978; Dickinson, 1979; Dickinson, 2004; Schwartz et al., 2010; LaMaskin et al., 2015), contains the eastern facies of deposition in the John Day region, separating it from the western facies in the adjacent high plains (Robinson et al., 1984) (**Figure 1B**). Today, the Blue Mountains create local gradients in precipitation and vegetation, with higher precipitation and a denser canopy in the mountain slopes (eastern facies) compared to the surrounding plains (western facies; **Figures 1C,D**). This significant local variability in hydroclimate and ecology may confound regional-scale interpretations of paleo archives if similar gradients existed in the past. For example, spatial variability can be misinterpreted as temporal variability if outcrop or sampling locations shift along these gradients with age. Similarly, changes in environmental parameters due to changes in local high elevation can be mis-attributed to the height of the Cascades if local topography is not accounted for.

There is some evidence that precipitation and vegetation gradients in the Blue Mountains have been present as far back as the Eocene. Near the western tip of the eastern facies Bestland and Retallack (1994) identified two different plant assemblages in the same stratigraphic horizon that point to distinct elevation regimes, perhaps related to Blue Mountain topography or local stratovolcanoes (White and Robinson, 1992). The floras are interpreted to reflect a wetter, more densely vegetated tropical lowland forest and an adjacent temperate, early successional highland forest (Bestland and Retallack, 1994; Bestland et al., 2002). In contrast, wetter conditions with denser vegetation appear in the highlands today while the lowlands are drier and sparsely vegetated (**Figures 1C,D**). Thus, while ecological gradients surrounding the Blue Mountains may be long-lived, their magnitude and even their direction may have changed with time.

In this study we present spatial and temporal oxygen isotope data from authigenic clay minerals, a proxy for past precipitation $\delta^{18}O$, to constrain the spatial expression of Blue Mountains topography and its effect on regional precipitation patterns. Isotopes of authigenic clays have been widely applied to studying tectonic and climatic change in Cenozoic western North America (Takeuchi and Larson, 2005; Mulch et al., 2006; Sjostrom et al., 2006; Mix et al., 2011, Mix et al., 2016, Mix et al., 2019; Chamberlain et al., 2012; Mix and Chamberlain, 2014) and they are particularly useful in places like John Day where soil carbonates—a more commonly used paleo-$\delta^{18}O$ proxy—are not continuously present through the sedimentary record (Bestland et al., 2002). Here, we document a ~3‰ offset in authigenic clay $\delta^{18}O$ between the western and eastern facies, with lower values in the east. This offset is best explained by the influence of the Blue Mountains on local precipitation patterns, indicating the range has supported local precipitation gradients since at least the Eocene.

GEOLOGIC SETTING

Prior to the deposition of Cenozoic sediment in the John Day region, the Mesozoic accretion of the Wallowa and Olds Ferry arcs created the Blue Mountains province (Dickinson and Thayer, 1978; Dickinson, 1979; Schwartz et al., 2010; LaMaskin et al., 2015). The province accreted along the Salmon River suture zone, likely sometime before 130 Ma (Dickinson, 1979, Dickinson, 2004; Schwartz et al., 2010; LaMaskin et al., 2015). After accretion, deformation of the suture zone is thought to have ended around 90 Ma, setting the stage for Cenozoic deposition within the John Day region.

Deposition in the John Day region occurred throughout the Eocene to the Pliocene and sediment was predominantly derived from air-fall ash and some ash-flow sheets with evidence for minor reworking by alluvial and lacustrine processes (Swanson and Robinson, 1968; Robinson et al., 1984; Graham, 2014). Volcanism appears frequent throughout the depositional record and likely shifted westward from the Blue Mountains province to the proto-Cascades ~37–40 million years ago, possibly due to "flat slab" detachment and a steepening of western North American subduction (Lipman et al., 1972; Noble, 1972; Robinson et al., 1984; Heller et al., 1987). This shift may be linked to the start of Western Cascades uplift, but early volcanism in the Western Cascades was likely associated with isolated stratovolcanoes along a low-lying coastal plain that may not have intercepted westerly moisture as effectively as today's Cascades Range (White and Robinson, 1992; Dillhoff et al., 2009). The timing of the onset of the Cascades rainshadow is still debated, and likely varies north-south (Priest, 1990; Kohn et al., 2002; Takeuchi and Larson, 2005; Takeuchi et al., 2010; Bershaw et al., 2020; Pesek et al., 2020), but drier, rainshadow-like conditions appear to emerge in Oregon in the late Oligocene to early Miocene (Woodburne and Robinson, 1977; MacFadden and Hulbert, 1988; Retallack, 2004).

The eastern and western facies of John Day deposition are separated by the Blue Mountains but they share some lithologic similarities (Swanson and Robinson, 1968; Robinson et al., 1984). The facies share the same formations for most of the Cenozoic, from the lower-mid Eocene Clarno Formation to the upper Eocene–lower Miocene John Day Formation. After deposition of the John Day Formation, the western facies contains the Ellensburg, Simtustus, Dalles, and Deschutes Formations while the eastern facies contains the Mascall and Rattlesnake Formations (Smiley, 1963; Farooqui et al., 1981; Smith, 1986; Graham, 2014). Both facies are primarily comprised of claystones and air-fall tuffs. The western facies contains more ash-flows and lava-flows than the eastern facies, suggesting a volcanic source west of the Blue Mountains and indicating the topographic barrier of the Blue Mountains may have limited the eastern extent of these deposits (Swanson and Robinson, 1968; Robinson et al., 1984). A third unit, referred to as the southern facies, also exists within the Blue Mountains region and shares lithological similarities with the eastern facies, but was not sampled in this study. The western facies, especially after the westward shift in volcanism at ~40 Ma, generally hosts coarser grained volcaniclastic material with thicker sedimentary packages, further supporting a western source of volcanic material (Robinson et al., 1984).

Paleobotanical evidence in the John Day region points to a long-term aridification trend beginning about 30 million years ago with the expansion of open-habitat grasslands. Paleosols at this time contain evidence for grassy root textures, and mammal fossils reveal adaptations for running ("cursoriality," a common indicator of open vegetation) and eating tougher foods like grasses ("hypsodonty") (MacFadden and Hulbert, 1988; Janis et al., 2002; Retallack, 2004). This transition to drier conditions, lasting until ~19 Ma, is generally interpreted to reflect strengthening of the Cascades rainshadow and/or a shift in the seasonality of precipitation from summer-dominated to the winter-dominated regime that exists today (Retallack, 2004; Retallack, 1997).

METHODS

Authigenic Clay Sample Preparation and Isotopic Analysis

We analyzed the oxygen isotope composition of 29 samples spanning 15 localities to build on existing data from Takeuchi (2007). Clay-rich paleosol samples were gently ground with a mortar and pestle and centrifuged to separate the <0.5 µm size fraction. The separated material was dried and gently ground with a mortar and pestle into a powder. Samples with indication of organic matter (dark coloration) were treated with a 3% hydrogen peroxide (H_2O_2) solution for 24–48 h before being rinsed at least 5 times with de-ionized water in a centrifuge.

At least one sample from each sedimentary package at each locality was run for X-ray diffraction to identify the clay mineralogy and screen for quartz. X-ray diffractometry was run at the Stanford University Environmental Measurements Facility using a Rigaku MiniFlex 600 Benchtop X-ray Diffraction System. The diffractometer is equipped with a copper (Cu) anode set at the maximum power of 600 W. Powdered samples were first suspended in isopropanol and left to air-dry on a zero-background quartz sample holder. Once dried, each sample was run twice with the 2-theta angle ranging from 2 to 90°. Samples were untreated in the first run and glycolated in the second run. To glycolate the samples, dried powders were placed in a sealed desiccator with 1 cm of ethylene glycol at the base and left overnight in an oven set to 65°C. The Rigaku PDXL software was used to aid in mineral identification for each sample. Samples identified to have quartz and/or illite peaks were not analyzed for oxygen isotopes.

After screening for quartz and illite, 1–2 mg of sample powder was mixed with lithium flouride (LiF; ~1:1 by mass) and pressed into pellets. The LiF pellets prevent dispersion of clay powder during laser ablation. Samples were brought to a vacuum to remove atmospheric vapor in the LiF. Any remaining vapor and any sorbed water in smectite minerals was removed through 2–4 pre-flourinations where samples were exposed to bromine pentaflouride (BrF_5) for ~90 s. Afterward, samples were laser ablated with a New Wave Research MIR10-25 infrared laser ablation system in the presence of BrF_5 to liberate O_2 gas (Sharp, 1990; Sjostrom et al., 2006; Mix and Chamberlain, 2014; Mix et al., 2016). Oxygen isotope analyses on O_2 gas were performed in dual-inlet mode at the Stanford University Stable Isotope Biogeochemistry Laboratory on a Thermo Finnigan MAT 252 or 253+, depending on the date of acquisition (Abruzzese et al., 2005; Hren et al., 2009; Mix et al., 2016; Chamberlain et al., 2020). We purified O_2 gas from samples run on the MAT 252 with two liquid nitrogen cold traps and one potassium bromide (KBr) trap before freezing O_2 on a liquid nitrogen-temperature zeolite and subsequently equilibrating it with the mass spectrometer sample bellows. On the MAT 253+, O_2 gas was purified with three liquid nitrogen traps and one sodium chloride ($NaCl$) trap, frozen on a zeolite at liquid nitrogen temperature, passed over a room temperature flow-through zeolite with high purity He as the carrier gas, and finally frozen in a zeolite trap and equilibrated with the mass spectrometer sample bellows. Repeated analyses of in-house standard DS069 were made during each day of analysis to correct for drift. Precision of DS069 replicates was 0.26‰ (n = 43). All isotopic ratios are reported relative to Vienna Standard Mean Ocean Water (VSMOW).

Comparing Oxygen Isotope Values of the Eastern and Western Facies

In order to map out the spatial pattern of authigenic clay $\delta^{18}O$ through the Cenozoic we calculate the residual of all data points relative to the Cenozoic trend. We build this Cenozoic trend by taking the average of the eastern and western facies trends, each defined by a loess smooth curve. This approach ensures that the Cenozoic trend is not biased toward one facies or the other when its sample density is relatively higher for a given point in time. After establishing the Cenozoic trend we calculate the residual $\delta^{18}O$ value for each sample ($\delta^{18}O_{sample} - \delta^{18}O_{trend}$). This represents a detrended record of $\delta^{18}O$ that allows for a spatial comparison of samples from different times of the record.

RESULTS

Most clay-size separates were comprised of smectite or mixed smectite/kaolinite with few kaolinite samples. Samples containing illite and/or quartz were not analyzed for $\delta^{18}O$. Kaolinite-rich samples are mostly found in the Eocene when conditions were likely wetter, consistent with the findings of Takeuchi (2007). Typical diffraction patterns for smectite, kaolinite, and excluded (illite/quartz) samples can be found in **Supplementary Figure S1**. We plot oxygen isotope data of kaolinite and smectite samples together because their fractionation factors are similar for at environmental temperatures (Sheppard and Gilg (1996); **Supplementary Figure S3**). We note that a recent database for oxygen isotope fractionation suggests a 2–3‰ offset between kaolinite and smectite fractionation at environmental temperatures (Vho et al., 2019), but the database is not recommended for use at low, environmental temperatures because a key approximation does not hold in this range Eq. 5 of Vho et al. (2019)).

Oxygen isotope values of our composite record range from 8.3 to 16.9‰ with an average value of 12.5‰ (±2.2‰, 1 σ). In the eastern facies the average $\delta^{18}O$ value is 11.1‰ (±1.9‰, 1 σ) and in the western facies mean $\delta^{18}O$ is 13.7‰ (±1.6‰, 1 σ). Throughout the record, oxygen isotope values in the eastern facies (the Blue Mountains province) are ~3‰ lower than those from the western facies, while $\delta^{18}O$ values in both facies follow similar trends. Specifically, eastern and western facies $\delta^{18}O$ values both show a ~3‰ increase between 30 and 20 Ma (**Figure 2A**).

DISCUSSION

Oxygen Isotopes of the Eastern and Western Facies

Lower oxygen isotope values in the Blue Mountains province (eastern facies) suggests this local topographic feature has

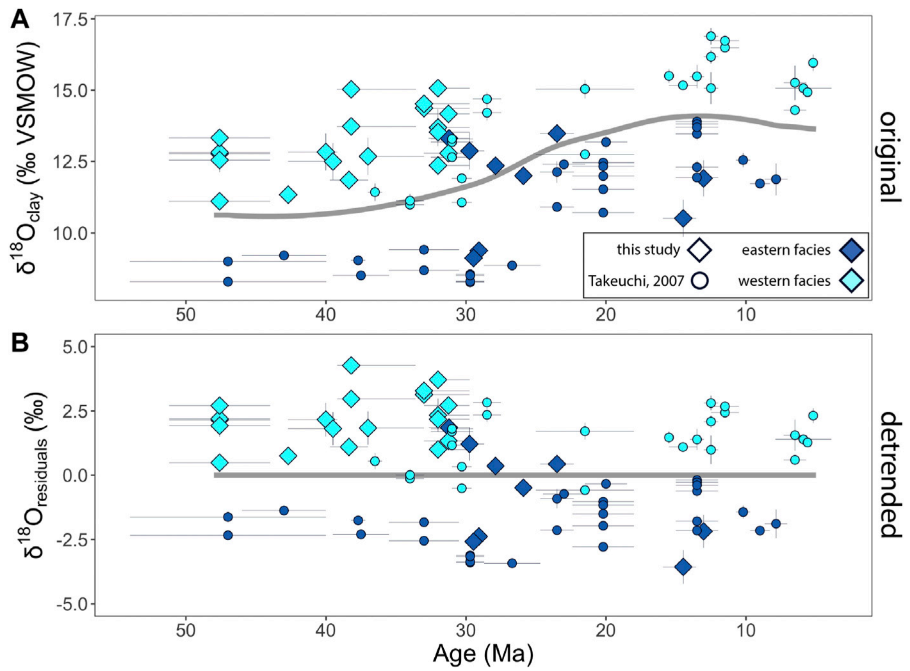

FIGURE 2 | (A) Oxygen isotope values of authigenic clay samples (‰ VSMOW) in the eastern (dark blue) and western (light blue) facies. Diamonds denote data from this study and circles are from Takeuchi (2007). In both panels the thin, horizontal and vertical gray lines are age uncertainty and $\delta^{18}O$ uncertainty, respectively. Thick, gray line denotes the average of the eastern and western facies trends, representing a regional trend. **(B)** Residual $\delta^{18}O$ values relative to the regional trend (gray line). Eastern facies $\delta^{18}O$ values are ~3‰ lower than the western facies throughout the record.

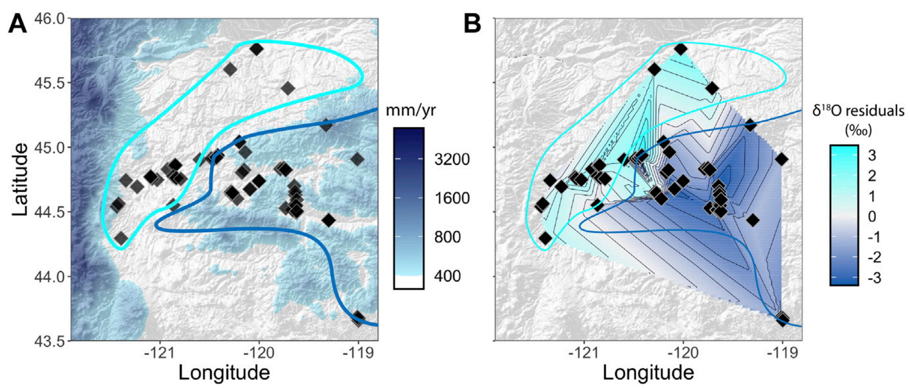

FIGURE 3 | (A) Zoomed-in panel (see **Figures 1B,C**) of sample locations (black diamonds) and mean annual precipitation. Light and dark blue polygon outlines reflect the approximate spatial extent of the western and eastern facies, respectively (after Albright et al. (2008); Graham (2014); Robinson et al. (1984); Takeuchi (2007)). **(B)** Spatially interpolated map of $\delta^{18}O$ residuals overlain with eastern and western facies extents.

influenced regional precipitation patterns for at least the last ~50 million years (Dickinson and Thayer, 1978; Dickinson, 1979; Schwartz et al., 2010; LaMaskin et al., 2015). Based on spatial interpolation of oxygen isotope residuals (**Figure 2B**) we find that the boundary between negative (lower $\delta^{18}O$) and positive (higher $\delta^{18}O$) residuals closely tracks the modern boundary of the eastern and western facies (which is, itself, defined by the extent of the Blue Mountains) (**Figure 3**). This close correspondence with the modern extent of the Blue Mountains suggests the possibility that authigenic clay $\delta^{18}O$ values reflect modern conditions due to diagenetic alteration or overprinting by modern waters instead of reflecting changes in past precipitation $\delta^{18}O$. However, $\delta^{18}O$ values from the eastern and western facies both increase by ~3‰ between 30 and 20 Ma, and this shift likely would not be coherent if all samples have been similarly altered by modern waters. Thus, we interpret $\delta^{18}O$ values to represent the oxygen isotope composition of water at the time of clay mineral formation.

Today, the windward slopes of the Blue Mountains capture more annual precipitation than the adjacent high plains (see

Figure 1C) and receive a larger fraction of annual precipitation during the winter months (**Supplementary Figure S2**). Both of these observations support lower $\delta^{18}O$ values in the Blue Mountains than in the adjacent plains. First, increased rainout over mountains is often explained by topography forcing air upward, leading to adiabatic cooling and moisture condensation and precipitation (Aristotle, 1931; Smith, 1979; Smith and Barstad, 2004; Roe, 2005). Higher precipitation due to Blue Mountains orography implies more rainout and a decrease in $\delta^{18}O$ values as precipitation preferentially removes $\delta^{18}O$. Alternatively, lower $\delta^{18}O$ values in the Blue Mountains region may be related to precipitation seasonality as, compared to the plains, the Blue Mountains receive a greater fraction of total precipitation in the winter months when precipitation $\delta^{18}O$ values are lower. It is possible that upslope rainout and precipitation seasonality both contribute to lower $\delta^{18}O$ values in the Blue Mountains. However, disentangling the effect of seasonality from upslope rainout on precipitation $\delta^{18}O$ is difficult because most modern $\delta^{18}O$ data in the John Day region are sampled in warmer months or from rivers that integrate seasonal precipitation (e.g., Bershaw et al. (2019)).

Despite the close link between residual $\delta^{18}O$ values and the extent of the Blue Mountains, $\delta^{18}O$ residuals do not correlate strongly with modern elevation or fraction of winter precipitation (**Supplementary Figure S4**). Residual $\delta^{18}O$ values generally decrease with elevation by ~3.3‰ per kilometer, similar to the regional lapse rate of ~3.2‰ Bershaw et al. (2020) per kilometer, but the correlation is weak ($R^2 = 0.17$). There is no significant correlation between residual $\delta^{18}O$ and the fraction of annual precipitation occurring in winter. The weak relationships between past clay $\delta^{18}O$ and modern conditions is not unexpected since some clays likely formed in contact with local meteoric water (tracking local elevation and precipitation seasonality) while others formed in floodplains in contact with upstream runoff (tracking the upstream hypsometric mean elevation and precipitation seasonality). Without reliable constraints on past floodplain extents and local drainage divides it is difficult to determine the relative importance of elevation, precipitation seasonality, or other factors in eastern and western facies $\delta^{18}O$ values. Additionally, modern winter precipitation and topography may differ from that of most samples in our record. Thermochronometry and geochronology data from the western Cascades in the latitude range of our samples points to exhumation between 20 and 10 Ma (Pesek et al., 2020), and there is abundant evidence that the timing of Cascades uplift and exhumation varied north-to-south (Reiners et al., 2002; Takeuchi and Larson, 2005; Pesek et al., 2020). If spatially variable topographic changes affected the spatial pattern of $\delta^{18}O$, a direct comparison of past John Day data with modern conditions may be invalid.

Implications for Regional Climate and Tectonics

Our results suggest that a regional gradient in precipitation amount and/or seasonality has existed around the Blue Mountains for most of the last 50 million years. If the Blue Mountains did not increase rainout or were not elevated above the plains, we would expect no difference in clay $\delta^{18}O$ values between the eastern and western facies. While the Blue Mountains are generally wetter than the adjacent plains today, lower $\delta^{18}O$ values in the eastern facies does not require that the Blue Mountains were wetter in the past. For example, it is possible that the Blue Mountains and the plains received similar amounts of annual precipitation, but summer (winter) precipitation made up a larger fraction of annual precipitation in the plains (mountains). However, summer and winter precipitation both increase with elevation in the Blue Mountains (and across the western United States; **Supplementary Figure S5**) today, and there is no clear reason why topography would not have the same effect on precipitation in the past. We suggest the Blue Mountains have received more precipitation than the surrounding plains for at least the last ~50 million years. Thus, a possible Eocene boundary between tropical lowland and temperate highland vegetation (Bestland and Retallack, 1994; Bestland et al., 2002) is likely driven by colder temperatures or topographic relief, but not drier conditions in the Blue Mountains.

Despite a long-lived precipitation gradient associated with the Blue Mountains, both the Blue Mountains and the plains record an increase in $\delta^{18}O$ values that tracks independent evidence for regional aridification. This $\delta^{18}O$ increase is probably not driven by temperature since the shift is unidirectional while global climate both warmed and cooled between 30 and 20 Ma (Zachos et al., 2001). Meanwhile, the onset of drier conditions between 30 and 20 million years ago is evidenced by the expansion of open-habitat grasslands and mammals adapted to running and eating tougher vegetation like grasses (Woodburne and Robinson, 1977; MacFadden and Hulbert, 1988; Jacobs et al., 1999; Janis et al., 2002; Retallack, 2004), although this transition may also be explained by grassland-grazer coevolution, independent of climate (Retallack, 2001; Retallack, 2013). The ~3‰ increase in authigenic clay $\delta^{18}O$ may be related to drying, but the interpretation is not straightforward. For example, Retallack (2004) suggests that drying is related to 1) the uplift of the Cascades and 2) a decrease in summer (high-$\delta^{18}O$) precipitation. But both of these effects would likely decrease $\delta^{18}O$ values rather than increase them. Further, marine $\delta^{18}O$ values vary by just 1‰ from 30 to 20 Ma and do not show a systematic increase capable of overprinting the effects of Cascades uplift and less summer precipitation (Zachos et al., 2001). Increased upstream (westward) moisture recycling in drier climates can also increase $\delta^{18}O$ (Salati et al., 1979; Sonntag et al., 1983; Mix et al., 2013; Chamberlain et al., 2014; Winnick et al., 2014; Kukla et al., 2019), but this effect is negligible in near-coastal settings where upstream land area is minimal (Mix et al., 2013; Winnick et al., 2014; Kukla et al., 2019).

Instead, we speculate that the $\delta^{18}O$ increase in our data reflects the onset of the Cascades rainshadow driving a decrease in winter (low-$\delta^{18}O$) precipitation. Today, the Cascades represent a much stronger rainshadow in the winter than in the summer (e.g., Siler and Durran (2016); **Supplementary Figure S6**), suggesting the possibility that their uplift would disproportionately decrease winter precipitation inland. Still, it is not clear that the increase in $\delta^{18}O$ from less winter precipitation could outweigh any decrease in $\delta^{18}O$ from Cascades uplift. It is possible that other factors associated with drier conditions, like surface water and subcloud evaporation, could also increase $\delta^{18}O$. Thus, more work is needed to test the hypothesis that drying in the John Day region is owed to disproportionate drying in the winter.

The distinct isotopic signature of the Blue Mountains emphasizes the importance of local elevation in regional tectonic reconstructions. Even though the eastern and western facies lie leeward (east) of the Cascades, lower $\delta^{18}O$ values in the eastern facies (the Blue Mountains) may be misinterpreted to reflect the height of the Cascades instead of local topography. For example, using hydrogen isotopes of a volcanic glass sample from the Blue Mountains, Bershaw et al. (2019) suggests the Cascades may have been higher than present as early as ~32 million years ago. Alternatively, we suggest that low hydrogen isotope ratios in the Oligocene reflect the local topography of the Blue Mountains rather than upstream elevation of the Cascades. Interestingly, the hydrogen isotope data of Bershaw et al. (2019) reveal an increase in δD of ~16‰ (~2‰ in $\delta^{18}O$) that happens near the mid-Miocene, between ~16 and 8 Ma, significantly later than the increase of ~3‰ between 30 and 20 Ma found in our data. Due to sparse hydrogen isotope data east of the Cascades older than 20 Ma, it is not clear whether volcanic glass δD also records an increase from 30 to 20 Ma. Further, while there are few coeval glass samples from the eastern and western facies to test for a spatial pattern, the existing data do not show a systematic difference in δD between the two regions. If the spatial and temporal trends of authigenic clay and volcanic glass isotopes differ, it is likely that the proxies are forming under different conditions and may be seasonally biased relative to one another. Such information would provide increasingly nuanced insight to the uplift history of the Cascades and its effect on leeward precipitation seasonality. However, at present there is not enough overlap between our authigenic clay data and the volcanic glass data to determine whether the results truly reflect distinct trends.

CONCLUSION

The Blue Mountains have likely supported local (<100 km) gradients in precipitation for much of the Cenozoic with more precipitation reaching the Blue Mountains than the surrounding plains. Distinct floral assemblages from the same stratigraphic interval provided the first hint that the John Day region may have hosted multiple biomes as early as the Eocene (Bestland and Retallack, 1994; Bestland et al., 2002), and our stable isotope results suggest these biomes could co-exist due to distinct elevation and climate regimes. We also find no evidence that regional drying from 30 to 20 million years ago was driven by a shift from summer-dominated to winter-dominated precipitation (Retallack, 2004).

Our high spatial resolution constraints on Blue Mountains topography provides a benchmark for future paleo -floral and -faunal work in the John Day region. Efforts to compare floral and faunal assemblages from the eastern and western facies will constrain how the Blue Mountains influenced local ecosystem dynamics through time. Additionally, our results suggest that the comparison of authigenic clay $\delta^{18}O$ and mammal tooth enamel $\delta^{18}O$ may allow for constraints on local mammal migration patterns. For example, comparing tooth enamel $\delta^{18}O$ from mammals of the same site may inform whether the range of some animals was more local than others (living in the eastern facies, western facies, or traveling between both). Further, changes in the inferred seasonal amplitude of tooth enamel $\delta^{18}O$ could reflect changes in seasonal migration between the two facies. Overall, our constraints on the spatial pattern of Blue Mountains topography and its possible influence over regional precipitation opens new opportunities for biogeography research on the relationship between landscapes and life in John Day through the Cenozoic.

DATA AVAILABILITY STATEMENT

The original contributions presented in the study are included in the article/**Supplementary Material**, further inquiries can be directed to the corresponding author.

AUTHOR CONTRIBUTIONS

TK, DI, JR, SK, and CC conceptualized the study. TK, DI, and CM performed laboratory analysis. TK, DI, JR, JG, DM, and CC performed fieldwork. JG and DM led field-based observation. TK analyzed data and wrote the original draft. All authors contributed to editing and revising.

FUNDING

This research was funded by NSF EAR-1322084 and Heising-Simons grants to CPC.

ACKNOWLEDGMENTS

The authors acknowledge J. Bershaw and Gregory Retallack for comments that improved the manuscript. We also acknowledge Joshua X. Samuels, Nicholas Famoso, Shelley Hall, and Patrick Gamman for assistance obtaining research permits at John Day Fossil Beds National Monument. We also thank Joshua X. Samuels for assistance with field stratigraphy and sampling, and Nicholas Famoso for further guidance on sampling and our age model. Elevation data are sourced from Terrain Tiles hosted on Amazon Web Services. Terrain Tiles data combines Global ETOPO1 and 3DEP datasets. Global ETOPO1 terrain data is courtesy of the U.S. National Oceanic and Atmospheric Administration. United States 3DEP (formerly NED) and global GMTED2010 and SRTM terrain data are courtesy of the U.S. Geological Survey. Research at John Day Fossil Beds National Monument was conducted under Study Number JODA-00033 with Permit Numbers JODA-2017-SCI-001 and JODA-2018-SCI-002, issued by John Day Fossil Beds and the United States Department of the Interior National Park Service.

SUPPLEMENTARY MATERIAL

The Supplementary Material for this article can be found online at: https://www.frontiersin.org/articles/10.3389/feart.2021.635181/full#supplementary-material.

REFERENCES

Abruzzese, M. J., Waldbauer, J. R., and Chamberlain, C. P. (2005). Oxygen and hydrogen isotope ratios in freshwater chert as indicators of ancient climate and hydrologic regime. *Geochem. Cosmochim. Acta* 69, 1377–1390. doi:10.1016/j.gca.2004.08.036

Albright, L. B., III, Woodburne, M. O., Fremd, T. J., Swisher, C. C., III, MacFadden, B. J., and Scott, G. R. (2008). Revised chronostratigraphy and biostratigraphy of the John Day Formation (Turtle cove and kimberly members), Oregon, with implications for updated calibration of the Arikareean North American land mammal age. *J. Geol.* 116, 211–237. doi:10.1086/587650

Aristotle (c 350 B.C.E., translated) (1931). *Meteorologica* Editor W. D. Ross Translated by E.W. Webster) (Oxford, UK: Oxford: Clarendon Press).

Bershaw, J., Cassel, E. J., Carlson, T. B., Streig, A. R., and Streck, M. J. (2019). Volcanic glass as a proxy for Cenozoic elevation and climate in the Cascade Mountains, Oregon, United States. *J. Volcanol. Geoth. Res.* 381, 157–167. doi:10.1016/j.jvolgeores.2019.05.021

Bershaw, J., Hansen, D. D., and Schauer, A. J. (2020). Deuterium excess and ^{17}O-excess variability in meteoric water across the Pacific Northwest, United States. *Tellus B* 72, 1–17. doi:10.1080/16000889.2020.1773722

Bestland, E., and Retallack, G. J. (1994). Geology and Palaeoenvironments of the Clarno unit (John Day Fossil Beds National Monument, Oregon: US National Park Service Open-File Report).

Bestland, E. A., Hammond, P. E., Blackwell, D. L. S., Kays, M. A., Retallack, G. J., and Stimac, J. (2002). Geologic framework of the Clarno unit, John Day fossil Beds National monument, Central Oregon (Oregon Department of Geology and Mineral Industries Open-File Report), 1–39.

Chamberlain, C., Ibarra, D., Lloyd, M., Kukla, T., Sjostrom, D., Gao, Y., et al. (2020). Triple oxygen isotopes of meteoric hydrothermal systems – implications for palaeoaltimetry. *Geochem. Perspect. Lett.* 15, 6–9. doi:10.7185/geochemlet.2026

Chamberlain, C. P., Mix, H. T., Mulch, A., Hren, M. T., Kent-Corson, M. L., Davis, S. J., et al. (2012). The cenozoic climatic and topographic evolution of the western north American Cordillera. *Am. J. Sci.* 312, 213–262. doi:10.2475/02.2012.05

Chamberlain, C. P., Winnick, M. J., Mix, H. T., Chamberlain, S. D., and Maher, K. (2014). The impact of neogene grassland expansion and aridification on the isotopic composition of continental precipitation. *Global Biogeochem. Cycles* 28, 992–1004. doi:10.1002/2014GB004822

Clark, R. D. (1989). *The Odyssey of Thomas Condon: Irish immigrant: frontier missionary: oregon geologist*. 1st Edn. Portland, OR: Oregon Historical Society.

Dickinson, W. R. (2004). Evolution of the North American Cordillera. *Annu. Rev. Earth Planet Sci.* 32, 13–45. doi:10.1146/annurev.earth.32.101802.120257

Dickinson, W. R. (1979). Mesozoic forearc basin in central Oregon. *Geology* 7, 166–170. doi:10.1130/0091-7613(1979)7<166:mfbico>2.0.co;2

Dickinson, W. R., and Thayer, T. P. (1978). "Paleogeographic and paleotectonic implications of Mesozoic stratigraphy and structure in the John Day Inlier of Central Oregon," in *Mesozoic paleogeography of the Western United States* (Los Angeles, California: Pacific Section: Society of Economic Paleontologists and Mineralogists), 147–161, no. 2 in Pacific Coast Paleogeography Symposium.

Dillhoff, R. M., Dillhoff, T. A., Dunn, R. E., Myers, J. A., and Stromberg, C. A. (2009). Cenozoic paleobotany of the John Day Basin, Central Oregon. *Geol. Soc. America Field Guide* 15, 165–185. doi:10.1130/2009.fl

Farooqui, S. M., Beaulieu, J. D., Bunker, R. C., Stensland, D. E., and Thoms, R. E. (1981). Dalles Group: neogene formations overlying the Columbia River Basalt Group in north-central Oregon. *Oregon Geol.* 43, 131–140.

Graham, J. P. (2014). John Day Fossil Beds national monument geologic resources inventory report, 117.

Heller, P. L., Tabor, R. W., and Suczek, C. A. (1987). Paleogeographic evolution of the United States Pacific Northwest during Paleogene time. *Can. J. Earth Sci.* 24, 1652–1667. doi:10.1139/e87-159

Hren, M. T., Tice, M. M., and Chamberlain, C. P. (2009). Oxygen and hydrogen isotope evidence for a temperate climate 3.42 billion years ago. *Nature* 462, 205–208. doi:10.1038/nature08518

Jacobs, B. F., Kingston, J. D., and Jacobs, L. L. (1999). The origin of grass-dominated ecosystems. *Ann. Mo. Bot. Gard.* 86, 590. doi:10.2307/2666186

Janis, C. M., Damuth, J., and Theodor, J. M. (2002). The origins and evolution of the North American grassland biome: the story from the hoofed mammals. *Palaeogeogr. Palaeoclimatol. Palaeoecol.* 177, 183–198. doi:10.1016/S0031-0182(01)00359-5

Kellndorfer, J., Walker, W., Kirsch, K., Fiske, G., Bishop, J., LaPoint, L., et al. (2012). NACP aboveground biomass and carbon baseline data (NBCD 2000). ORNL DAAC.

Kohn, M. J., and Fremd, T. J. (2007). Tectonic controls on isotope compositions and species diversification, John Day Basin, central Oregon. *PaleoBios* 27, 14.

Kohn, M. J., Miselis, J. L., and Fremd, T. J. (2002). Oxygen isotope evidence for progressive uplift of the Cascade Range, Oregon. *Earth Planet Sci. Lett.* 204, 151–165. doi:10.1016/S0012-821X(02)00961-5

Kukla, T., Winnick, M. J., Maher, K., Ibarra, D. E., and Chamberlain, C. P. (2019). The sensitivity of terrestrial δ^{18}O gradients to hydroclimate evolution. *J. Geophys. Res.: Atmos.* 124, 563–582. doi:10.1029/2018JD029571

LaMaskin, T. A., Dorsey, R. J., Vervoort, J. D., Schmitz, M. D., Tumpane, K. P., and Moore, N. O. (2015). Westward growth of Laurentia by Pre–Late jurassic terrane accretion, Eastern Oregon and Western Idaho, United States. *J. Geol.* 123, 233–267. doi:10.1086/681724

Lipman, P. W., Prostka, H. J., and Christiansen, R. L. (1972). Cenozoic volcanism and plate-tectonic evolution of the Western United States. I. Early and middle cenozoic. *Phil. Trans. Math. Phys. Eng. Sci.* 271, 217–248. doi:10.1098/rsta.1972.0008

MacFadden, B. J., and Hulbert, R. C. (1988). Explosive speciation at the base of the adaptive radiation of Miocene grazing horses. *Nature* 336, 466–468. doi:10.1038/336466a0

Merriam, J. C., and Sinclair, W. J. (1906). *Tertiary faunas of the John Day region*. University of California Publications on Geological Sciences, Vol. 5, 171–205.

Mix, H. T., and Chamberlain, C. P. (2014). Stable isotope records of hydrologic change and paleotemperature from smectite in Cenozoic western North America. *Geochem. Cosmochim. Acta* 141, 532–546. doi:10.1016/j.gca.2014.07.008

Mix, H. T., Caves Rugenstein, J. K., Reilly, S. P., Ritch, A. J., Winnick, M. J., Kukla, T., et al. (2019). Atmospheric flow deflection in the late Cenozoic Sierra Nevada. *Earth Planet Sci. Lett.* 518, 76–85. doi:10.1016/j.epsl.2019.04.050

Mix, H. T., Ibarra, D. E., Mulch, A., Graham, S. A., and Page Chamberlain, C. (2016). A hot and high Eocene Sierra Nevada. *Bull. Geol. Soc. Am.* 128, 531–542. doi:10.1130/B31294.1

Mix, H. T., Mulch, A., Kent-Corson, M. L., and Chamberlain, C. P. (2011). Cenozoic migration of topography in the North American Cordillera. *Geology* 39, 87–90. doi:10.1130/G31450.1

Mix, H. T., Winnick, M. J., Mulch, A., and Page Chamberlain, C. (2013). Grassland expansion as an instrument of hydrologic change in Neogene western North America. *Earth Planet Sci. Lett.* 377–378, 73–83. doi:10.1016/j.epsl.2013.07.032

Mulch, A., Graham, S. A., and Chamberlain, C. P. (2006). Hydrogen isotopes in Eocene river gravels and paleoelevation of the Sierra Nevada. *Science* 313, 87–89. doi:10.1126/science.1125986

Noble, D. (1972). Some observations of the cenezoic volcano-tectonic evolution of the great Basin, Western United States. *Earth Planet Sci. Lett.* 17, 142–150. doi:10.1016/0012-821x(72)90269-5

Pesek, M. E., Perez, N. D., Meigs, A., Rowden, C. C., and Giles, S. M. (2020). Exhumation timing in the Oregon cascade range decoupled from deformation, magmatic, and climate patterns. *Tectonics* 39, e2020TC006078. doi:10.1029/2020TC006078

Priest, G. R. (1990). Volcanic and tectonic evolution of the cascade volcanic Arc, Central Oregon. *J. Geophys. Res.* 95, 19583–19599. doi:10.1029/JB095iB12p19583

Reiners, P. W., Ehlers, T. A., Garver, J. I., Mitchell, S. G., Montgomery, D. R., Vance, J. A., et al. (2002). Late Miocene exhumation and uplift of the Washington cascade range. *Geology* 30, 767–770. doi:10.1130/0091-7613(2002)030<0767:lmeauo>2.0.co;2

Retallack, G. J. (2001). Cenozoic expansion of grasslands and climatic cooling. *J. Geol.* 109, 407–426. doi:10.1086/320791

Retallack, G. J. (2013). Global cooling by grassland soils of the geological past and near future. *Annu. Rev. Earth Planet Sci.* 41, 69–86. doi:10.1146/annurev-earth-050212-124001

Retallack, G. J. (2004). Late Oligocene bunch grassland and early Miocene sod grassland paleosols from central Oregon, United States. *Palaeogeogr., Palaeoclimatol., Palaeoecol.* 207, 203–237. doi:10.1016/S0031-0182(04)00042-2

Retallack, G. J. (1997). Neogene expansion of the North American Prairie. *Palaios* 12, 380–390. doi:10.2307/3515337

Retallack, G. J., Wynn, J. G., and Fremd, T. J. (2004). Glacial-interglacial-scale paleoclimatic change without large ice sheets in the Oligocene of central Oregon. *Geology* 32, 297–300. doi:10.1130/G20247.1

Robinson, P. T., Brem, G. F., Mckee, E. H., Survey, U. S. G., Road, M., Park, M., et al. (1984). John Day Formation of Oregon: a distal record of early cascade volcanism. *Geology* 12, 229–232. doi:10.1130/0091-7613(1984)12<229

Robson, S., Famoso, N., Davis, E., and Hopkins, S. (2019). First mesonychid from the Clarno Formation (Eocene) of Oregon, United States. *Palaeontol. Electron.* 22, 1–13. doi:10.26879/856

Roe, G. H. (2005). Orographic precipitation. *Annu. Rev. Earth Planet Sci.* 33, 645–671. doi:10.1146/annurev.earth.33.092203.122541

Salati, E., Dall'Olio, A., Matsui, E., and Gat, J. R. (1979). Recycling of water in the Amazon Basin: an isotopic study. *Water Resour. Res.* 15, 1250–1258. doi:10.1029/WR015i005p01250

Samuels, J. X., Albright, L. B., and Fremd, T. J. (2015). The last fossil primate in North America, new material of the enigmatic Ekgmowechashala from the Arikareean of Oregon. *Am. J. Phys. Anthropol.* 158, 43–54. doi:10.1002/ajpa.22769

Schwartz, J. J., Snoke, A. W., Frost, C. D., Barnes, C. G., Gromet, L. P., and Johnson, K. (2010). Analysis of the Wallowa-Baker terrane boundary: implications for tectonic accretion in the Blue Mountains province, northeastern Oregon. *Geol. Soc. Am. Bull.* 122, 517–536. doi:10.1130/B26493.1

Sharp, Z. D. (1990). A laser-based microanalytical method for the *in situ* determination of oxygen isotope ratios of silicates and oxides. *Geochem. Cosmochim. Acta* 54, 1353–1357. doi:10.1016/0016-7037(90)90160-M

Sheppard, S., and Gilg, H. (1996). Stable isotope geochemistry of clay minerals. *Clay Miner.* 31, 1–24. doi:10.1180/claymin.1996.031.1.01

Siler, N., and Durran, D. (2016). What causes weak orographic rain shadows? insights from case studies in the Cascades and idealized simulations. *Am. Meteorol. Soc.* 73, 4077–4099. doi:10.1175/JAS-D-15-0371.1

Sinclair, W. J. (1905). *New or imperfectly known rodents and ungulates from the John Day Series*. Berkeley, CA: University of California Publications on Geological Sciences, Vol. 4, 125–143.

Sjostrom, D. J., Hren, M. T., Horton, T. W., Waldbauer, J. R., and Chamberlain, C. P. (2006). Stable isotopic evidence for a pre–late Miocene elevation gradient in the Great Plains–Rocky Mountain region, United States. *Geol. Soc. Am. Spec. Pap.* 398, 309–319. doi:10.1130/2006.2398(19)

Smiley, C. (1963). *The Ellensburg flora of Washington*. Berkeley, CA University of California Publications on Geological Sciences, Vol. 35, 159–276.

Smith, G. A. (1986). Simtustus Formation: paleogeographic and stratigraphic significance of a newly defined Miocene unit in the Deschutes basin, central Oregon. *Oregon Geol.* 48, 63–72.

Smith, R. B. (1979). "The influence of mountains on the atmosphere," in *Advances in geophysics*, Editor B. Saltzman (New York, NY: Elsevier).

Smith, R. B., and Barstad, I. (2004). A linear theory of orographic precipitation. *J. Atmos. Sci.* 61, 1377–1391. doi:10.1175/1520-0469(2004)061<1377:altoop>2.0.co;2

Sonntag, C., Rozanski, K., Münnich, K., and Jacob, H. (1983). "Variations of deuterium and oxygen-18 in continental precipitation and groundwater and their causes," in *Variations in the Global Water Budget*, Editors A. Street-Perrott, M. Beran, and R. Ratcliffe (D. Reidel Publishing Company), 107–124.

Swanson, D., and Robinson, P. (1968). *Base of the John Day Formation in and near the Horse Heaven mining district, north-central Oregon*. Washington, D.C.: U.S. Geological Survey Professional Paper, 154–161.

Takeuchi, A. (2007). Decoupling the ancient hydrologic system from the modern. Thesis.

Takeuchi, A., and Larson, P. B. (2005). Oxygen isotope evidence for the late Cenozoic development of an orographic rain shadow in eastern Washington, United States. *Geology* 33, 313–316. doi:10.1130/G21335.1

Takeuchi, A., Hren, M. T., Smith, S. V., Chamberlain, C. P., and Larson, P. B. (2010). Pedogenic carbonate carbon isotopic constraints on paleoprecipitation: evolution of desert in the Pacific Northwest, United States, in response to topographic development of the Cascade Range. *Chem. Geol.* 277, 323–335. doi:10.1016/j.chemgeo.2010.08.015

Vho, A., Lanari, P., and Rubatto, D. (2019). An internally-consistent database for oxygen isotope fractionation between minerals. *J. Petrol.* 60, 2101–2129. doi:10.1093/petrology/egaa001

White, J. D., and Robinson, P. T. (1992). Intra-arc sedimentation in a low-lying marginal arc, Eocene Clarno Formation, central Oregon. *Sediment. Geol.* 80, 89–114. doi:10.1016/0037-0738(92)90034-O

Winnick, M. J., Chamberlain, C. P., Caves, J. K., and Welker, J. M. (2014). Quantifying the isotopic 'continental effect'. *Earth Planet Sci. Lett.* 406, 123–133. doi:10.1016/j.epsl.2014.09.005

Woodburne, M. O., and Robinson, P. T. (1977). A new late hemingfordian mammal fauna from the John Day Formation, Oregon, and its stratigraphic implications. *J. Paleontol.* 51, 750–757.

Zachos, J., Pagani, M., Sloan, L., Thomas, E., and Billups, K. (2001). Trends, rhythms, and aberrations in global climate 65 Ma to present. *Science* 292, 686–693. doi:10.1126/science.1059412

Conflict of Interest: The authors declare that the research was conducted in the absence of any commercial or financial relationships that could be construed as a potential conflict of interest.